



Alexandria University  
**Alexandria Engineering Journal**

[www.elsevier.com/locate/aej](http://www.elsevier.com/locate/aej)  
[www.sciencedirect.com](http://www.sciencedirect.com)



# Novel adaptation of Marston's stress solution for inclined backfilled stopes

Walid El Kamash <sup>a,\*,1</sup>, Hany El Nagggar <sup>b</sup>, Sivakugan Nagaratnam <sup>c</sup>

<sup>a</sup> Department of civil engineering, suez canal university, Ismailia 41522, Egypt

<sup>b</sup> Department of Civil and Resource Engineering, Dalhousie University, Nova Scotia B3H 4R2, Canada

<sup>c</sup> College of Science & Engineering, James Cook University, Townsville, Australia

Received 26 May 2021; revised 31 December 2021; accepted 21 January 2022

## KEYWORDS

Mine stopes;  
 Backfills;  
 Stress distribution;  
 Marston's formula

**Abstract** In underground mining, it is crucial to consider the arching phenomenon, especially for inclined backfilled trenches and mine stopes. That phenomenon decreases the vertical stress of the fill material, so, the in-site stress has already redistributed itself to the hanging- and foot-walls when the stope was excavated. In such cases, the mobilized resistance due to friction between the granular backfill material and the inclined walls can substantially reduce the pressure at the bottom of the stope, which could have a major impact on the stability of the backfill medium and consequently also on economic aspects. Most of researchers used numerical analysis or Lab. tests to predict both of vertical and lateral stresses in inclined stopes. However, there is a need to investigate analytical solution to describe the behaviour of those stresses in inclined stopes. Based on Marston's formula, this research provides a new approach to predicting vertical stresses at any depth in inclined backfilled stopes. The proposed approach introduces a new parameter,  $\eta$ , to account for the contribution of backfill arching. This parameter specifies the ratio of normal stresses on the hanging wall and foot wall of the inclined backfilled stope. This differs from previous approaches, which assumed that the normal stress on the inclined backfilled stope's hanging wall and foot wall was equal. To validate the proposed approach, results obtained are compared with numerical, analytical, and experimental results from previous research. It is found that if the proposed parameter,  $\eta$ , is modified to 0.2 for the lateral earth pressure coefficient at rest with an angle of inclination of 60° to 80°, good agreement with experimental data is achieved.

© 2022 Production and hosting by Elsevier B.V. on behalf of Faculty of Engineering, Alexandria University. This is an open access article under the CC BY-NC-ND license (<http://creativecommons.org/licenses/by-nc-nd/4.0/>).

\* Corresponding author.

E-mail addresses: [waleedkamash@eng.suez.edu.eg](mailto:waleedkamash@eng.suez.edu.eg) (W.E. Kamash), [hany.elnagggar@dal.ca](mailto:hany.elnagggar@dal.ca) (H.E. Nagggar), [siva.sivakugan@jcu.edu.au](mailto:siva.sivakugan@jcu.edu.au) (S. Nagaratnam).

<sup>1</sup> Visiting research academic, James Cook University, Townsville, Australia.

Peer review under responsibility of Faculty of Engineering, Alexandria University.

<https://doi.org/10.1016/j.aej.2022.01.058>

1110-0168 © 2022 Production and hosting by Elsevier B.V. on behalf of Faculty of Engineering, Alexandria University.

This is an open access article under the CC BY-NC-ND license (<http://creativecommons.org/licenses/by-nc-nd/4.0/>).

## 1. Introduction

Mine stopes are frequently not completely vertical or horizontal but may be inclined at an angle. For this reason, an accurate estimation of the vertical stress plays an important role in the economics of the mining industry. The arching phenomenon reduces vertical stress; thus, a consideration of this

phenomenon can be of value for many applications, including underground pipes and containers for storing compact granular materials such as chemical powders, tablets, caplets, cement, and flour.

Suggesting an analytical formula in a simple form can therefore be very helpful for the design of such applications. In this research, based on the assumption that the stope walls serve as boundary constraints that cause the arching effect, theoretical expressions are used to estimate vertical and horizontal stresses at any depth of the backfilled stope. Previous formulas are based on the principle of the shear plane, where the forces involved are in equilibrium in the state of balance which considers that both orthogonal reactions on hang wall and foot wall are equivalent. This study proposes the ratio of normal stresses on the hanging wall and footwall (HW/FW) as an innovative aspect and key input value for estimating stress in inclined walls. That ratio is denoted as  $\eta$ . In addition, appropriate values for lateral earth pressure are studied, focusing on the coefficients  $K_a$ ,  $K_o$  and  $K_{af}$ . Mining plays an important economic role in many countries, including Australia, Canada and United States. Ore can be extracted via open cut mining or underground mining, where the walls can be vertical or inclined. Rocks should be restored again to their open trench after extracting the ore. The stability of those returned rocks can be a big problem and causes many accidents specially in Australia. This paper investigates vertical pressures in underground mining in cases where the walls of underground spaces are inclined. In the mining industry, the use of inappropriate methods in the backfilling of tailings can lead to the failure of barricades and subsequent stopes, if many large underground drives are involved. There is thus an urgent need for geotechnical solutions in the mining industry to support the production of minerals in situations where crushed rocks are extracted.

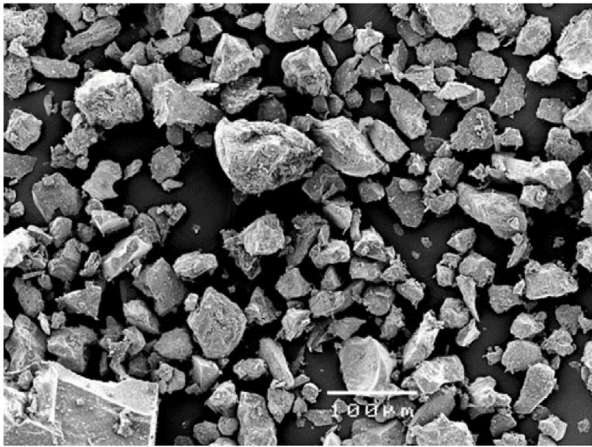
Stopes with vertical or inclined walls can be identified as rectangular trenches. The typical height/width ratio of stopes in Australia can range from 4 to 6; for example, with a height of 200 m and a width of 40 to 50 m. It should be noted that stopes are connected to horizontal access drives located at various sublevels, which allow the movement of trucks and other equipment. Before stopes are backfilled, they are generally first blocked by barricades made of bricks or concrete. Thus, it is important to predict both the vertical stress at the bottom of backfilled stopes and the horizontal stress acting on the block material of the barricades. Crushed rock from mine tailings can be used in underground mines to fill multiple stopes. The distribution of grain size is a significant factor that affects the properties of tailings used for backfilling. Backfills range from granular materials which is focused in this study such as rock, concrete and sand, to solid materials as in the case of hydraulic or paste filling.

El Kamash et al. [7] presented a numerical research to assess the true value of the normal stress ratio at the hung wall to the foot-wall. The effect of arching between the backfill and the inclined walls is taken into account. The results are compared with experimental evidence and with solutions that are available in the literature. Adoko et al. [1] suggested a methodology for measuring stope overbreak and dilution. They proposed the FFN-based classifier as a tool to supplement the traditional stability graph method in open stope design. Using three stress scenarios, Saedi et al. [30] demonstrated that,

despite the development of large brittle and tensile degradation zones within the rock mass, no substantial brittle or tensile breakdown is envisaged at the proposed mining levels. The geomechanical behaviour of waste rock barricades in interaction with mine backfill was researched by Nujaim et al. [24]. They demonstrated that the barricade's stability is determined by its physical features as well as the frictional behaviour at the barricade/drift wall interface. Villalba and Kumral [39] introduced a three-stage stochastic optimization model that incorporates genetic algorithms (GA) to account for grade uncertainty. The stope layout uncertainty was determined in the first stage, while the second stage breeds the initial population by creating average designs and evaluating their viability, and the third stage employs GAs to improve this initial population across generations. Vallejos et al. [38] presented three-dimensional numerical models for developing new induced stress curves and assessing their influence on the stability graph approach and open stope mine design. The findings revealed that there were significant variances in the predicted stresses at the stopes' walls, resulting in an increase in the stopes' size. Sivakugan and Widisinghe [33] presented a scanning electron micrograph of a sample of hydraulic fill, shown in Fig. 1a.

Most of the material found in tailings is crushed rock with angular shapes that can result in a large friction angle between the backfill and the stope wall. The water content of hydraulic fill can be increased to facilitate the transport of fill in stopes. For this reason, most barricades are constructed of porous material or are equipped with drainpipes. As shown in Fig. 1b, Ting et al. [36] provided an image of a barricade constructed of blocks, prior to the stope filling phase. One of the most complex problems facing the mining industry is the failure of barricades due to construction that does not adequately consider the principles of geotechnical engineering. Such failures can result in significant financial losses and closing of the mine. In this analysis, to simplify the problem, it is assumed that the granular fill is in a dry condition. This assumption has been widely used in related backfill stress studies for inclined stopes, for example in Li et al. [14], Pirapakaran and Sivakugan (2003), and Pirapakaran and Sivakugan (2007). Wide underground spaces are created during the mining process, which can be regarded as roughly vertical or rectangular trenches that required backfilling.

Stope backfilling improves regional stability in the mine, so that ore can be extracted from adjacent sites. It is also an effective way to dispose of tailings since broken waste rock tailings can be recycled as backfill materials. Barricades are used to safeguard horizontal access drives, as adjacent stopes are filled. Unfortunately, the collapse of barricades is an ongoing problem, resulting in dangerous accidents in the mining world. To improve understanding of the effective loads on barricades, there should be a focus on the role of stress arching for decreasing vertical stresses in mine stopes. Although Marston and Anderson [21] observed a vertical stress asymptote with depth in trench backfills, it should be kept in mind that filling with granular material would involve no significant cohesion, causing the vertical stresses to vary from the equation suggested by Marston and Anderson [21]. Handy [10] suggested that a catenary-shaped arch forms a minor principal direction in a horizontal layer. Singh et al. [31] also developed an analytical equation for calculating the vertical stress at a point, by using a circular arch for the lower main stress. In addition,



(a)



(b)

**Fig. 1** (a) Scanning electron micrograph of sample of hydraulic fill [33]; (b) Construction of a barricade [36].

Singh et al. [31] showed that the effect of considering minor principal stress directions as a circular or catenary aspect of a horizontal layer is negligible.

Due to the arching phenomenon, the granular material in a backfilled stope generates a lateral pressure on the rock walls. The lateral stress produced can be caused by the presence of a non-cohesive material which expands laterally until the slope balance is reached at an angle equal to the angle of rest. Thus, the rock walls confine the granular material, serving as boundary constraints that represent the response of the material stress. In other words, the stope rock walls represent a rough confinement system that develops shear strength due to friction between the walls and backfill. The shear strength acts as a reaction in the opposite direction of the weight of the material and its surcharge, resulting in a reduction of the vertical stress on the bottom. In the case of inclined mine stopes, the backfill interaction is restricted to two walls, the lower of which is the footwall (FW), while the upper wall is referred to as the hanging wall (HW). Ting et al. [36] have shown that there is a major difference between the vertical and inclined load distribution profiles, although the arching effect is reduced by the inclination of the walls. Many researchers, such as Mitchell et al.

[23], Aubertin et al. [2], Li et al. [16,17], Pirapakaran and Sivakugan [25–27], and Li and Aubertin [18] are focusing on studying the stress distribution and arching mechanism inside backfilled stopes. Jahns and Brauner (via [13] argued that vertical stresses in stopes inclined at an angle of  $30^\circ$  to the vertical vary from those in vertical stopes by no more than 10%. However, Li and Aubertin [15,19] suggested that to prevent significant differences, vertical stopes should be considered as an approximation for inclined stopes only in the case of inclined stopes deviating by no more than  $10^\circ$  from the vertical.

In theory, the lateral pressure coefficient within a soil mass is defined for a single level. However, the ratio of the horizontal stress on the wall to the average vertical stress at the bottom is represented by  $K$  in classical equations and is not specified at a single level. The lateral pressure coefficient at rest,  $K_0$ , was defined by Bishop [3] as the ratio of lateral to vertical effective stresses in a soil consolidated under the condition of no lateral deformations. The stresses involved are principal stresses without shear stress applied to the planes on which these stresses function. El-Sohby and Andrawes [8] updated this description to eliminate historical implications by expressing the ratio of horizontal to vertical stress in terms of stress increases. A numerical modelling approach was suggested as an effective method for the design of a paste fill bulkhead [6]. When the problem situation is complex and three-dimensional, it is not feasible to obtain accurate estimates of theoretical solutions. In addition, due to difficulties in obtaining vertical stress measurements in situ for this type of backfill situation, numerical simulations can offer an alternative for estimating the lateral variance of vertical stresses. When a drive and barricade are introduced, this becomes a three-dimensional problem which would be difficult to simplify into a two-dimensional framework. Nevertheless, Li and Aubertin [15] and Fahey et al. [9] modelled the stress condition near a barricade in plane strain with two-dimensional numerical sets, assuming a uniformly distributed drive along the bottom of the stope. To analyse load variations, Revell and Sainsbury [29] performed simulations by using three-dimensional numerical barricade models with backfilling. The degree of arching is an aspect of shear stress mobilisation. The reduction of pressure due to arching varies with height, or more precisely with the ratio of height to width. Arching significantly affects the stress conditions in backfilled stopes. Often the vertical stress is reduced by 29.5 percent of the total overload stress in narrow stopes [9], and by as much as 60 percent of the overload stress in circular stopes [25]. It should be noted that Janssen (1895) developed the principle of arching for the prediction of stresses in powder silos (Sperl 2006). Marston [20] used the arching theory to consider stresses in buried pipelines (Whidden 2009).

To estimate the vertical stress inside inclined backfilled stopes, this paper derives an innovative formula-based analytical expression from Marston [20] that just describes vertical mining stopes. That novel research, which gives an analytical formula for estimating vertical stresses in inclined mine stopes, has an economic impact on this industry and can be considered an alternate solution to the numerical solution on the one hand. Most earlier approaches assumed that the typical stress on the hanging wall is the same as the normal stress on the foot wall, resulting in erroneous results. This proposed formula introduces a new parameter,  $\eta$ , which represents the ratio of normal stresses on the hanging wall and footwall (HW/FW), in this study. This new parameter,  $\eta$ , was added into the

analytical formula to accurately forecast vertical stresses in sloped mine stopes, giving designers a simple and safe method.

## 2. Proposed Marston modified approach

The definition of the first Marston model refers to the global stability of layer elements, as shown in Fig. 2. Based on this definition, the equation for predicting stress in a long vertical trench [22,2], and [11] was developed as follows.

$$\sigma_{vH} = \frac{\gamma B}{2K \tan \phi} \left\{ 1 - \exp\left(-\frac{2KH \tan \phi}{B}\right) \right\} \quad (1)$$

$$\sigma_{hH} = \frac{\gamma B}{2 \tan \phi} \left\{ 1 - \exp\left(-\frac{2KH \tan \phi}{B}\right) \right\} \quad (2)$$

where  $\sigma_{vH}$  and  $\sigma_{hH}$  are normal vertical and horizontal stresses at depth  $H$ ,  $\gamma$  is the unit weight of the backfill,  $B$  is the trench width,  $\phi$  is the friction angle of the backfill, and  $K$  is the ratio of normal horizontal stress to normal vertical stress. Rankine's active earth pressure coefficient,  $K_a$ , is defined as follows for backfill in an active state:

$$K = K_a = \tan^2(45^\circ - \phi/2) \quad (3)$$

For the case of backfilled openings (stopes, trenches, silos and even retaining wall), the confining structures exist first and the backfill is placed later. The state of the backfill after its placement is unknown. It can be in an active state [34] or in a state of at-rest as [40], depending on the values of the backfill's friction angle and Poisson's ratio [41].

Since the backfill is in a state of rest,  $K$  may be taken as the coefficient of earth pressure at rest,  $K_o$ . Jaky [12] suggested the following formula for  $K_o$ , the coefficient of earth pressure at rest:

$$K = K_o = 1 - \sin \phi \quad (4)$$

Based on Marston [20], a theoretical model is proposed here, developed as an improvement of the conventional theory of arching. The following assumptions were made:

- The walls confining the backfill are parallel and inclined.
- The vertical stress pattern at any depth is uniform.
- The stope is studied as a two-dimensional plane strain problem.

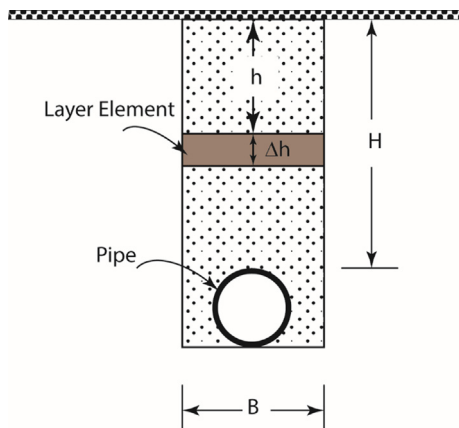


Fig. 2 Marston's layout for a conduit buried in a trench.

- The rock wall is very rough and therefore the friction between the rock face and the backfill is close to the friction in the backfill.
- The normal stress at the hanging wall (HW) is lower than the normal stress at the footwall (FW) and thus the shear stresses at the interfaces of these walls are different.

Fig. 3 shows a schematic diagram of a narrow stope with parallel inclined walls, which can be treated as a two-dimensional plane strain problem. The stope height is  $H$ , the width is  $L_B$ , and the stope walls are inclined relative to the horizontal at an angle of inclination  $\alpha$ . The symbol  $W$  denotes the weight of the layer component, while  $V$  and  $V + dV$  represent the vertical forces due to the fill load at the top and bottom of the significantly reduced layer with thickness  $\Delta h$ . The force perpendicular to the footwall-backfill interface is  $N$ , while  $S$  represents the shear force perpendicular to  $N$  along the wall. The normal and shear forces on the hanging wall are taken as  $\eta N$  and  $\eta S$ , where  $\eta$  is a reduction factor that is less than 1.

The weight,  $W$ , of the finite layer of thickness  $dh$  can be defined as follows:

$$W = \gamma(L_B)\Delta h \quad (5)$$

where  $h$  is the depth below the surface and  $\Delta h$  is the height of the discrete layer element. The following formula may be obtained by applying the equilibrium conditions for the discrete layer element and considering the vertical forces:

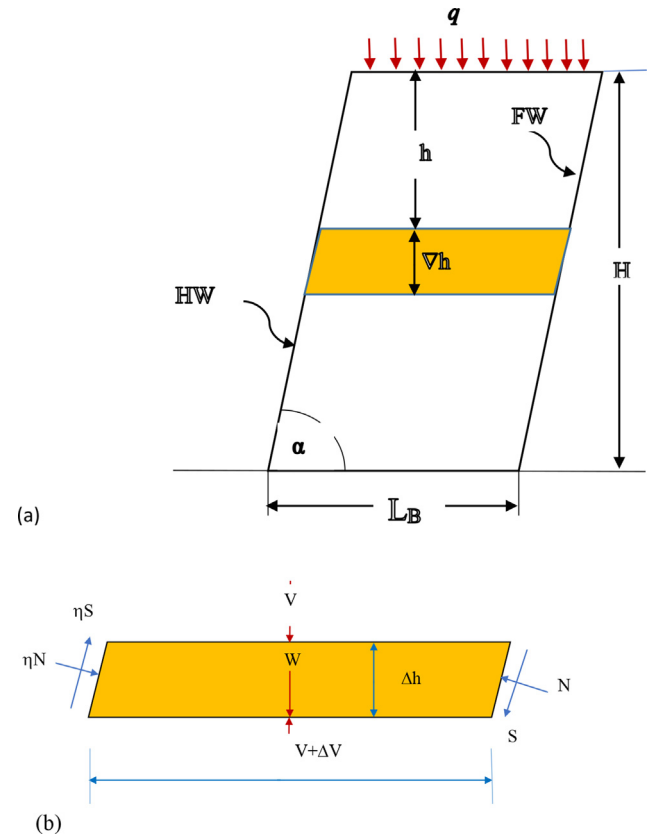


Fig. 3 (a) Stope with inclined parallel walls; (b) Free body diagram of a horizontal element of thickness  $\Delta h$ .

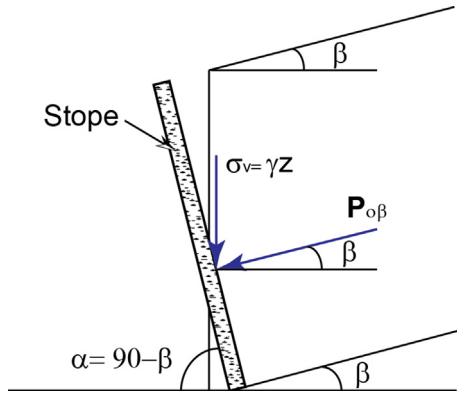


Fig. 4 Lateral earth pressure at rest.

$$W + V = (V + dV) + N \cos(\alpha) - \eta N \cos(\alpha) + S \sin(\alpha) + \eta S \sin(\alpha) \quad (6)$$

$$0 \leq \eta \leq 1$$

For a unit width of footwall, the normal forces  $N$  and  $S$  shown in Fig. 3b can be expressed as follows:

$$N = \sigma_n \frac{\Delta h}{\sin \alpha} \quad (7)$$

$$S = \sigma_n \frac{\Delta h}{\sin \alpha} \tan \delta \quad (8)$$

where  $\sigma_n$  is the normal stress on the plane of the inclined footwall, and  $\delta$  is the angle of friction of the interface between the wall and the backfill, which typically varies in the range of 0 to  $\phi$ , depending on the wall roughness.

The force  $V$  at depth  $h$ , shown in Fig. 3b, can be written as follows:

$$V = \sigma_v(L_B) \quad (9)$$

where  $\sigma_v$  is the normal vertical stress at depth  $h$ , which is assumed to be constant in the horizontal direction, so that  $dV$  can be expressed as:

$$dV = L_B d\sigma_v \quad (10)$$

By substituting Eqs. (5), (7), (8), (9) and (10) in Eq. (6), the following is obtained:

$$\begin{aligned} \gamma L_B \Delta h + \sigma_v L_B &= \sigma_v L_B + L_B d\sigma_v + \left(\sigma_n \frac{\Delta h}{\sin \alpha}\right) \cos(\alpha) \\ &\quad - \eta \left(\sigma_n \frac{\Delta h}{\sin \alpha}\right) \cos(\alpha) + \left(\sigma_n \frac{\Delta h}{\sin \alpha} \tan(\delta)\right) \\ &\quad \times \sin(\alpha) + \eta \left(\sigma_n \frac{\Delta h}{\sin \alpha} \tan(\delta)\right) \sin(\alpha) \end{aligned} \quad (11)$$

Dividing by  $(L_B \cdot \Delta h)$  then results in:

$$\begin{aligned} \gamma &= \frac{d\sigma_v}{\Delta h} + \frac{\left(\sigma_n \frac{\Delta h}{\sin \alpha}\right) \cos(\alpha)}{L_B \Delta h} - \eta \frac{\left(\sigma_n \frac{\Delta h}{\sin \alpha}\right) \cos(\alpha)}{L_B \Delta h} \\ &\quad + \frac{\left(\sigma_n \frac{\Delta h}{\sin \alpha} \tan(\delta)\right) \sin(\alpha)}{L_B \Delta h} + \eta \frac{\left(\sigma_n \frac{\Delta h}{\sin \alpha} \tan(\delta)\right) \sin(\alpha)}{L_B \Delta h} \end{aligned} \quad (12)$$

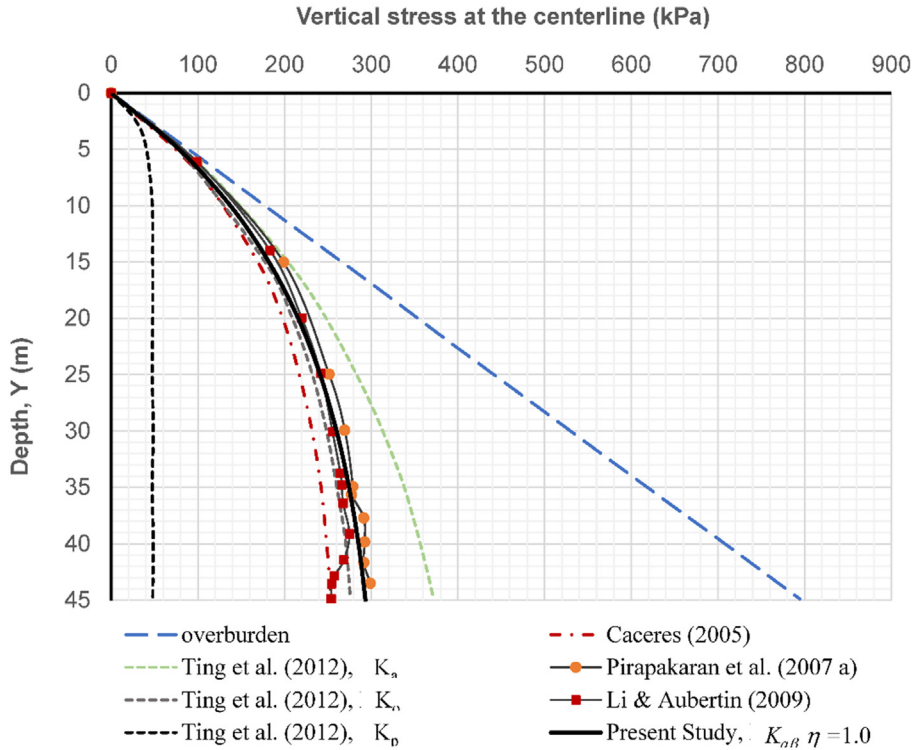


Fig. 5 Comparison of vertical stress along the vertical centreline of the stope; note that  $L_B = 6$  m,  $H = 45$  m,  $\gamma = 18$  kN/m<sup>3</sup>,  $c = 0$ ,  $\phi = 30^\circ$ ,  $\delta = 2/3 \phi$ ,  $q = 0$ , and  $\alpha = 90^\circ$ .

Eq. (12) can be rewritten as:

$$\frac{d\sigma_v}{\Delta h} = \gamma - \Psi\sigma_v \quad (13)$$

where the parameter  $\Psi$  is calculated according to:

$$\psi = \frac{K_x}{L_B \tan \alpha} \cdot [\eta(\tan \alpha \tan \delta - 1) + (1 + \tan \alpha \tan \delta)] \quad (14)$$

where  $K_x$  is defined as:

$$K_x = \frac{\sigma_n}{\sigma_v} \quad (15)$$

Thus,

$$\int_q^{\sigma_v} \frac{d\sigma_v}{\gamma - \Psi\sigma_v} = \int_0^h \Delta h \quad (16)$$

The differential Eq. (13) can be readily solved by numeric integration based on the Runge-Kutta method. The integral method must specify the boundary conditions, which in this case can be considered as  $\sigma_v = q$  at  $h = 0$ , where  $q$  is the stress of the surcharge. Thus,  $d\sigma_v/\Delta h$  can easily be obtained at the initial boundary of  $h = 0$  by substituting  $\sigma_v = q$  and  $h = 0$  in Eq. (13), as follows.

$$\text{at } h = 0, \frac{d\sigma_v}{\Delta h} = \gamma - \Psi(q) \quad (17)$$

Eq. (13) can be written in the following form, based on the Runge-Kutta equation.

$$\sigma_{v_{n+1}} = \sigma_{v_n} + \frac{1}{6}(k_1 + 2k_2 + 2k_3 + k_4) \quad (18)$$

If there is a surcharge, the initial value of  $\sigma_{v_n}$  can be replaced by  $q$ , otherwise it will be 0. Here  $k_1, k_2, k_3$  and  $k_4$  can be determined as follows:

$$k_1 = \varepsilon f(h_n, (\sigma_v)_n) \quad (19a)$$

$$k_2 = \varepsilon f\left(h_n + \frac{\varepsilon}{2}, (\sigma_v)_n + k_1/2\right) \quad (19b)$$

$$k_3 = \varepsilon f\left(h_n + \frac{\varepsilon}{2}, (\sigma_v)_n + k_2/2\right) \quad (19c)$$

$$k_4 = \varepsilon f(h_n + \varepsilon, (\sigma_v)_n + k_3) \quad (19d)$$

where  $h_{n+1} = h_n + \varepsilon$ , with  $h_0 = 0$  at initial zero depth conditions. Here  $\varepsilon$ , defined as a step-size expression of the accuracy of the solution, is taken to be 0.1 m, while  $n$  is defined as an integer incremental variable equal to 0,1,2,3, . . . . .

### 3. Lateral earth pressure coefficient

There are several ways to describe the lateral earth pressure in mine fill. These include the use of active and at-rest earth pressure parameters, the lower and upper bound methods, limit analyses, and plasticity-based characteristic systems. Marston's approach involves the Rankine active earth pressure coefficient,  $K_a$ , which is given by the following equation:

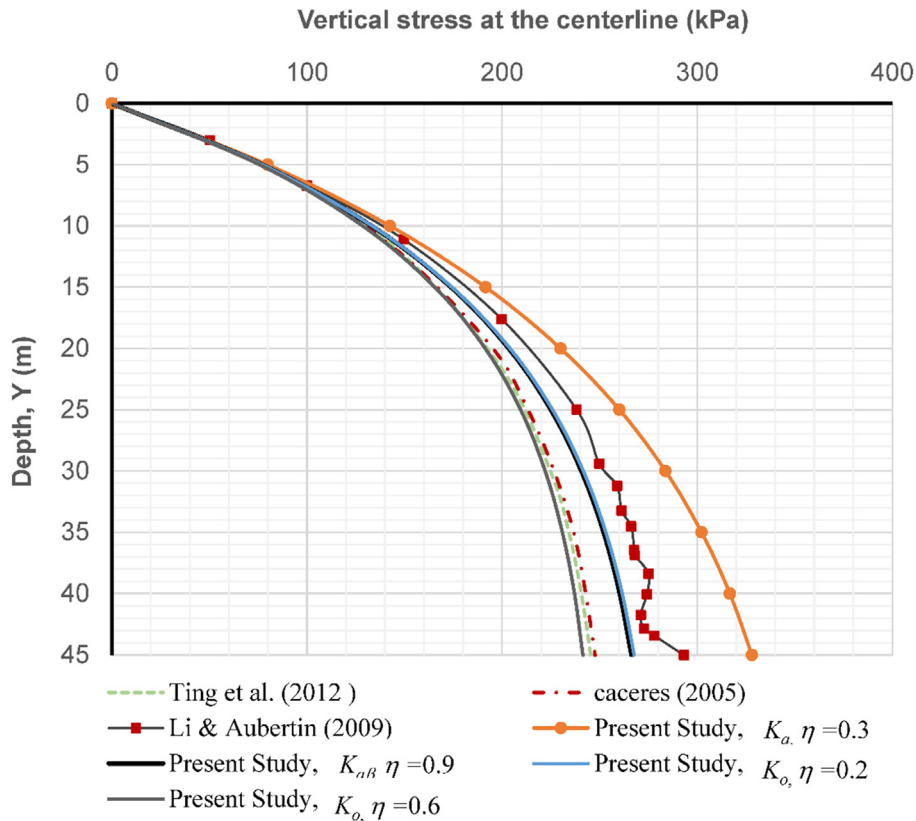


**Fig. 6** Comparison of vertical stress along the slope vertical centreline for different values of  $\eta$ ; note that  $L_B = 6$  m,  $H = 45$  m,  $\gamma = 18$  kN/m<sup>3</sup>,  $c = 0$ ,  $\phi = 30^\circ$ ,  $\delta = 2/3\phi$ ,  $q = 0$ , and  $\alpha = 80^\circ$ .

$$K_a = \tan^2\left(45 - \frac{\phi}{2}\right) = \frac{1 - \sin\phi}{1 + \sin\phi} \quad (20)$$

where  $\phi$  is the friction angle of the backfill. When the walls are very rough, this is the same as the friction angle of the wall-fill interface,  $\delta$ . It is suggested that  $\delta = \phi$  be used, as indicated in [32]. *Krynine* (1945) proposed that  $K$  could be taken as follows:

$$K_{Krynine} = \frac{1}{1 + 2\tan^2\phi} = \frac{1 - \sin^2\phi}{1 + \sin^2\phi} \quad (21)$$

Jaky [12] proposed the following coefficient,  $K_o$ , for earth pressure at rest:

$$K_o = 1 - \sin\phi \quad (22)$$

Most previous earth pressure coefficients have been derived based on the assumption that the horizontal and vertical vectors are perpendicular to one another. In contrast, here the angle between the horizontal and vertical stress vectors,  $\sigma_n$  and  $\sigma_v$ , can be denoted as  $\beta$  where  $\beta = 90 - \alpha$  and  $\alpha$  is the angle of inclination of the stope walls. *Bowels* [4] and *Terzaghi* [35] suggested a lateral earth pressure equation for a vertical retaining wall with backfill inclined at an angle  $\beta$ . In this case, between the vectors of lateral earth pressure,  $\sigma_n$ , and vertical pressure,  $\sigma_v$ , there is an angle equal to  $90 - \beta$ . The proposed Rankine earth pressure coefficient can therefore be formulated as follows, assuming a cohesionless backfill with  $c = 0$ .

$$K_{o\beta} = \frac{\cos\beta - \sqrt{\cos^2\beta - \cos^2\phi}}{\cos\beta + \sqrt{\cos^2\beta - \cos^2\phi}} \quad (23)$$

Based on the *Danish Geotechnical Institute* (1985), for a vertical wall retaining sloping ground, the coefficient of earth pressure at rest,  $k_{o\beta}$ , can be calculated from the following equation:

$$k_{o\beta} = (1 - \sin\phi')(1 + \sin\beta) \quad (24a)$$

where  $\beta$  is the slope angle of the earth, which has a positive value when the backfill slopes upward. Here the earth pressure at rest  $P_{o\beta}$  operates in a direction similar to the surface of the ground and can be assumed to increase linearly with depth:

$P_{o\beta} = k_{o\beta}\gamma z / \cos\beta$ . This can be developed as  $P_{o\beta} = K_{o\beta}\sigma_v$ , where  $K_{o\beta} = \frac{k_{o\beta}}{\cos\beta}$  and  $\sigma_v = \gamma z$ .

Assuming that the lateral ground pressure coefficient at slope  $\beta$  is identical to the case of the coefficient of lateral earth pressure at rest in inclined stopes,  $K_{o\beta}$ , as shown in Fig. 4, the  $K_{o\beta}$  of a stope with an inclination angle of  $(90 - \beta)$  with the horizontal plane can be formulated as follows:

$$K_{o\beta} = \frac{(1 - \sin\phi)(1 + \sin\beta)}{\cos\beta} \quad (24b)$$

In the case of a very rough wall,  $\delta$  is considered to be equal to  $\phi$  as follows.

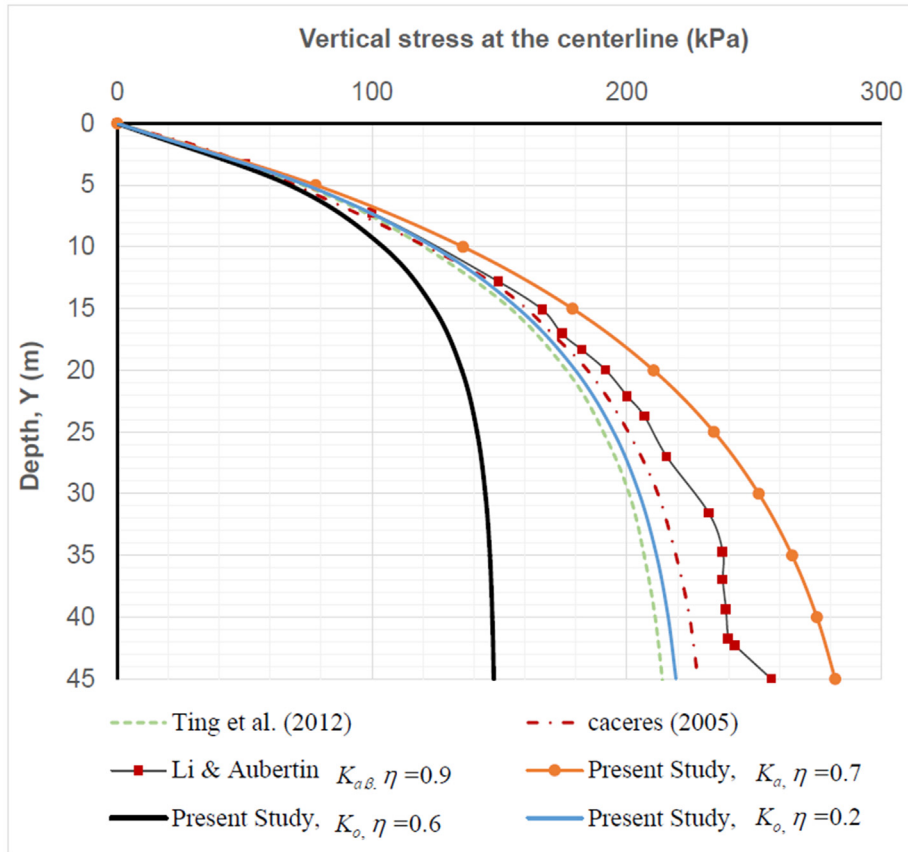


**Fig. 7** Comparison of vertical stress along the stope vertical centreline for different values of  $\eta$ ; note that  $LB = 6$  m,  $H = 45$  m,  $\gamma = 18$  kN/m<sup>3</sup>,  $c = 0$ ,  $\phi = 30^\circ$ ,  $\delta = 2/3\phi$ ,  $q = 0$ , and  $\alpha = 70^\circ$ .

$$K_{o\beta} = \frac{(1 - \sin\delta)(1 + \sin\beta)}{\cos\beta} \quad (24c)$$

For a wall which is less rough, Sivakugan and Widisinghe [33] suggest that  $\delta$  be within the range of 0.5 to 0.7 times  $\phi$ . When the earth is horizontal, it can be considered that  $\beta = 0^\circ$ . For the case of the vertical wall,  $\alpha = 90^\circ - \beta = 90^\circ$ , where  $K_{o\beta}$  is  $1 - \sin\phi$ . This should be close to  $K_o$  in Eq. (22) where, given a wall that is very rough,  $\delta = \phi$ .

#### 4. Verification of proposed modified approach

Here results of the modified Marston approach proposed in this study are compared with numerical results provided by Li and Aubertin [15,19], the analytical equation proposed by Caceres [5], and the analytical equation proposed by Ting et al. [36].

Figs. 5–8 compare results for the vertical stress at the centerline obtained via the proposed approach with results from the previous analytical solutions of Ting et al. [36] and Caceres [5] and the numerical analysis of Li and Aubertin [15,19]. It can be seen that the proposed parameter  $\eta$  contributes flexibility to the present approach, allowing it to be adopted for previous data for any angle of inclination. It should be noted that the use of  $K = K_o$  and  $\eta = 0.2$  results in strong agreement with previous results.

In a comparison with previous evidence provided by Ting et al. [36], Fig. 9 shows how the new updated method proposed in this study fits with previous findings. It should be noted that when  $K = K_o$  and  $\eta = 0.2$ , there is a strong agreement with the data provided by Ting et al. [36].

In addition, the comparison was expanded to include experimental laboratory data reported by Ting et al. [37]. These researchers performed a laboratory experiment with a physical model of an inclined slope, where a high-precision load cell was used to measure the fraction of the self-weight carried by the two walls. As well, strain gauges were used at the footwall to distinguish the components supported by the hanging wall and the footwall. The strain gauge readings thus represent measurements of distributed point loads, as illustrated in Fig. 10.

Sivakugan and Widisinghe [33] indicate that for granular soils, the parameter  $\delta$  should be 0.5 to 0.7 times  $\phi$  in the case of walls that are not very rough. Rankine et al. [28] reported that the friction angle  $\phi$  could be considered as  $19Dr^2 + 33$ , and that the angle  $\phi$  could be taken as  $40^\circ$  for a relative density of 60%. The interface friction angle parameter  $\delta$  is thus considered to be equivalent to  $r\phi$ , with values of  $r = 0.15, 0.5$  and  $1$  for cases of low, medium and high wall roughness, respectively.

Fig. 11 compares results of the solution proposed in this study with laboratory test results provided by Ting et al.

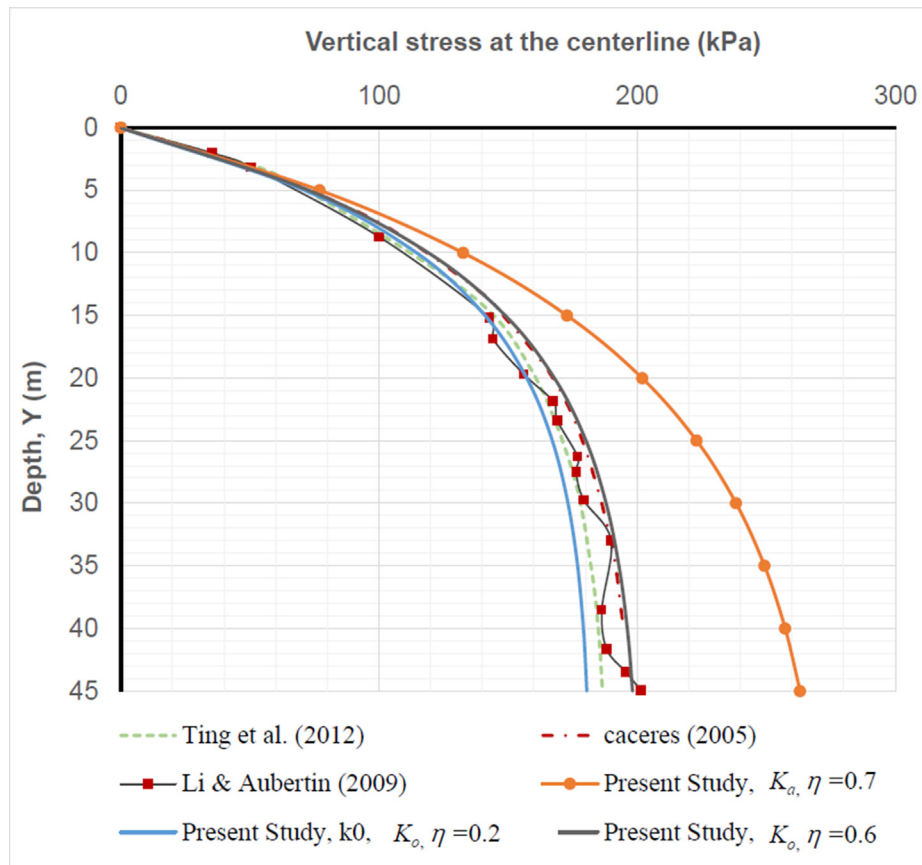


**Fig. 8** Comparison of vertical stress along the slope vertical centreline for different values of  $\eta$ ; note that  $LB = 6$  m,  $H = 45$  m,  $\gamma = 18$  kN/m<sup>3</sup>,  $c = 0$ ,  $\phi = 30^\circ$ ,  $\delta = 2/3\phi$ ,  $q = 0$ , and  $\alpha = 60^\circ$ .

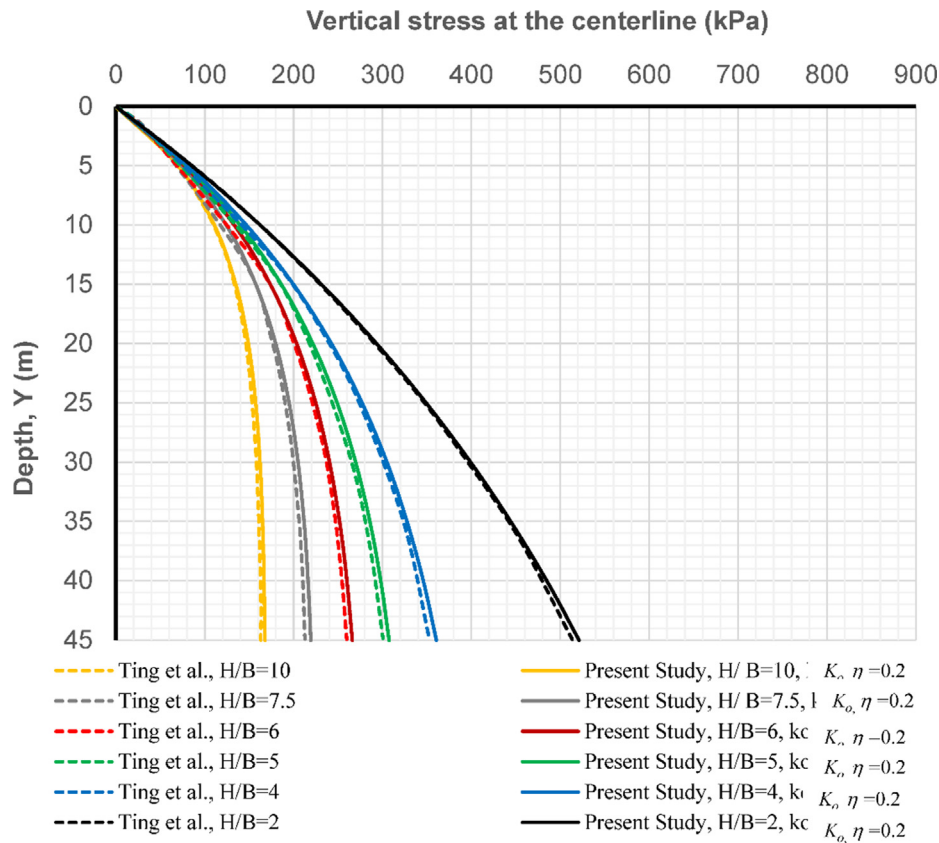


**Fig. 9** Comparison of vertical stresses along the vertical centreline for specific stope aspect ratios, with  $\eta = 0.2$ ; note that  $H = 45$  m,  $\gamma = 18$  kN/m<sup>3</sup>,  $c = 0$ ,  $\phi = 30^\circ$ ,  $\delta = 2/3\phi$ ,  $q = 0$ , and  $\alpha = 70^\circ$ .

[37]. The laboratory results were reported based on the relative backfill density, which is dependent on the internal friction angle of the backfill. In addition, low, medium and high wall roughnesses were used, which are associated with different interface friction angles. The  $\delta$  and  $\phi$  values were established by Sivakugan and Widinghe [33] and Rankine et al. [28], respectively.

The results show reasonable agreement for different height/width ratios, with an angle of inclination of  $70^\circ$ . Cases with different interface angle of friction,  $\delta$ , which represent high and low roughness are illustrated in Figs. 11 and 12, respectively.

The comparison was expanded to include three interface friction cases: low, medium, and high roughness, with inclination angles of  $80^\circ$  and  $90^\circ$ , as shown in Figs. 13 and 14, respectively. The results were generated as normalised values of  $\sigma_v/\gamma H$  versus height/width ( $z/B$ ). It should be noted that for an inclination angle of  $80^\circ$ , as shown in Fig. 13, there was good agreement for the case of low wall roughness, with some variance for medium and high roughness. As shown in Fig. 14, the deviation increased for an inclination angle of  $90^\circ$ . This may be because the interface friction angle should not be taken as a fraction of the internal friction angle.

## 5. Discussion of the parametric study results

The effects of the parameters  $\eta$  (the ratio of normal stresses on the hanging wall and footwall, HW/FW), and the coefficient of

lateral earth pressure,  $K$ , need to be well understood. The parameter  $\eta$  determines the normal response stress contribution of the inclined hanging wall and footwall. This parameter is directly influenced by the angle of inclination,  $\alpha$ . In order to understand the limits of the parameter  $\eta$ , let us assume a stope with an angle of inclination of  $0^\circ$ , which leads to a single reaction at the footwall, while the reaction at the hanging wall is zero; consequently  $\eta = 0$ . Thus  $\eta$  will be greater than 0 for an inclined stope with an angle of inclination of  $\alpha$  greater than  $0^\circ$ , until  $\eta$  becomes 1 at  $\alpha = 90^\circ$ . In the case of inclined stopes, the coefficient of lateral earth pressure,  $K$ , which characterizes the ratio of orthogonal vertical and horizontal stresses, is not a valid parameter because the angle between the vertical stress and the usual stress in an inclined stope is not  $90^\circ$ . Thus, the two parameters  $\eta$  and  $K$  may significantly affect the arching phenomenon. Their influence is examined below for different height/width aspect ratios, and for various internal and interface friction angles. The results are presented with standardised values for both axes.

### 5.1. The influence of $\eta$ on normalised vertical stress

Fig. 15 shows the effect of adjusting the value of  $\eta$  on the normalised vertical stress for different stope angles of inclination, with  $K = K_o$ . It can be observed in Fig. 15 that as the angle of inclination  $\alpha$  decreases, the effect of changing the value of  $\eta$  decreases until  $\alpha = 55^\circ$ , where the value of  $\eta$  ceases to have an effect (see Fig. 15a). As can be seen in Fig. 15b, c and d,



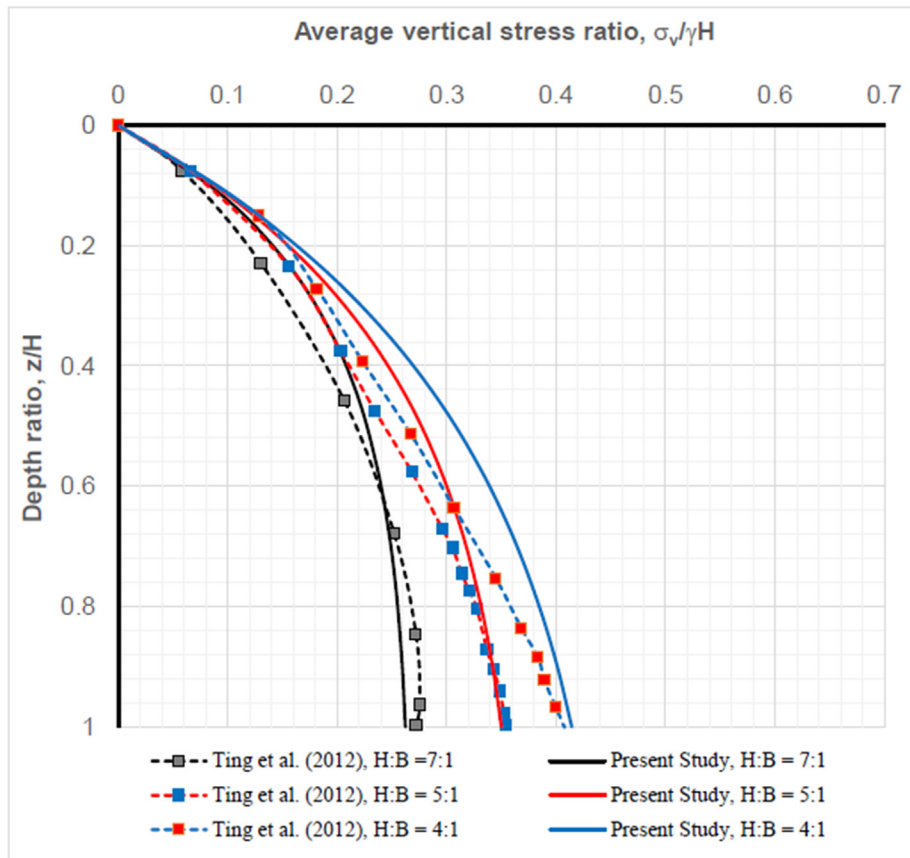


**Fig. 11** Comparison of vertical stresses along the vertical centreline for specific slope aspect ratios (note that the model has high roughness, with a relative density of 60% and  $\alpha = 70^\circ$ ; in the present study  $K_o$  and  $\eta = 0.6$  were used, with  $\phi = 40^\circ$  and  $\delta = \phi$  (high roughness)).

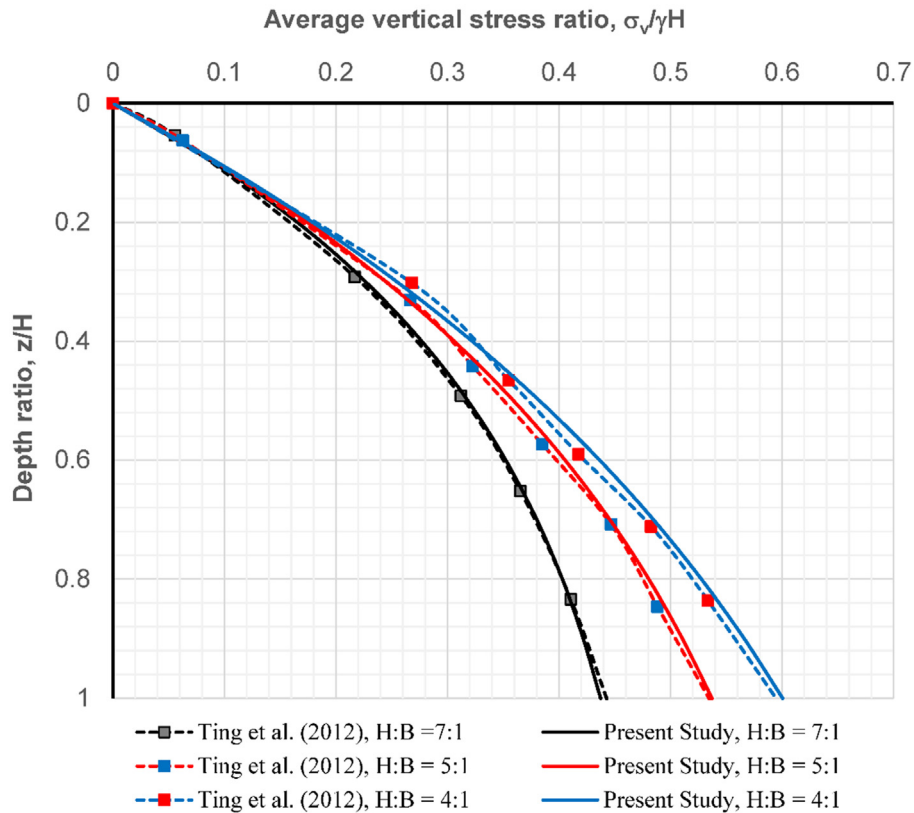
the replacement of  $K_o$  by  $K_a$ , the maximum difference between the vertical stresses attributable to different values of  $\eta$  (ranging from 0 to 1) is slightly reduced to 1.14, 1.30 and 1.48 at  $\alpha = 65^\circ$ ,  $\alpha = 75^\circ$  and  $\alpha = 85^\circ$ , respectively. As shown in Fig. 16a, changing the value of  $\eta$  has no effect at  $\alpha = 55^\circ$ .

Fig. 17 shows the effect of changing the value of  $\eta$  on the normalised vertical stress for different slope angles of inclination, with  $K = K_{a\alpha}$ . As can be seen in Fig. 17b, c and d, due to the replacement of  $K_o$  by  $K_{a\alpha}$ , the maximum difference between the vertical stresses attributable to different values of  $\eta$  (ranging from 0 to 1) is reduced to 1.17, 1.33 and 1.49 at  $\alpha = 65^\circ$ ,  $\alpha = 75^\circ$  and  $\alpha = 85^\circ$ , respectively. As shown in Fig. 17a, changing the value of  $\eta$  has no effect at  $\alpha = 55^\circ$ .

### 5.2. The influence of $K$ on normalised vertical stress

For any depth  $z$ , the parameter  $K$  can be defined as the ratio between the normal stresses perpendicular to the inclined wall at that point, and the corresponding vertical stress at the bottom of the slope. Various  $K$  coefficients have been suggested

by researchers, including  $K_o$ ,  $K_p$ ,  $K_a$  and  $K_{a\beta}$ . For inclined slopes,  $K$  is not well understood, because in this case the parameter  $K$  does not characterize the ratio between two perpendicular vectors. Fig. 18 shows the effect of using three different proposed  $K$  parameters:  $K_o$ ,  $K_a$  and  $K_{a\beta}$  on the determination of standardised vertical stress, with different angles of inclination and  $\eta = 0.5$ . Maximum and minimum vertical stresses can be observed. The use of  $K_a$  yielded the maximum  $\sigma_v$  at all angles of inclination,  $\alpha$ . Although the use of  $K_{a\beta}$  yielded the minimum  $\sigma_v$  for  $\alpha = 55^\circ$ , the use of  $K_o$  resulted in the minimum  $\sigma_v$  for all angles of inclination greater than  $55^\circ$ . It was found that for any inclined slope,  $K$  has no influence on the normalised vertical stress if the height/width ( $z/B$ ) ratio is less than 1. At any angle of inclination,  $\alpha$ , as the  $z/B$  ratio increases, the effect of  $K$  also increases. However, unlike the situation with the parameter  $\eta$ , the influence of  $K$  on the normalised vertical stress decreases as the angle of inclination increases. As shown in Fig. 18a, for  $\alpha = 55^\circ$ , the use of  $K_{a\beta}$ ,  $K_o$  and  $K_a$  yielded maximum standardised vertical stresses of 0.1, 0.24 and 0.35, respectively. Although the use of differ-



**Fig. 12** Comparison of vertical stresses along the vertical centreline for specific slope aspect ratios (note that the model has low roughness, with a relative density of 60% and  $\alpha = 70^\circ$ ; in the present study  $K_o$  and  $\eta = 0.6$  were used, with  $\phi = 40^\circ$  and  $\delta = 0.15\phi$  (Low roughness)).

ent  $K$  parameters yields significantly different normalised vertical stresses at lower angles of inclination, an increase in the angle of inclination reduces this effect. As shown in Fig. 18b, for  $\alpha = 65^\circ$ , the use of  $K_o$ ,  $K_{a\beta}$ , and  $K_a$  yielded maximum  $\sigma_v/\gamma H$  values of 0.26, 0.27 and 0.37, respectively. In Fig. 18c it can be seen that for  $\alpha = 75^\circ$ , the use of  $K_o$ ,  $K_{a\beta}$ , and  $K_a$  yielded maximum  $\sigma_v/\gamma H$  values of 0.27, 0.36 and 0.4, respectively; whereas Fig. 18d shows that for  $\alpha = 85^\circ$ , values obtained with the use of  $K_{a\beta}$ , and  $K_a$  mostly coincide, with  $K_o$ ,  $K_{a\beta}$ , and  $K_a$  yielding maximum values of 0.29, 0.42 and 0.42, respectively. The difference in normalised vertical stress due to the use of different  $K$  parameters thus reaches its maximum at  $\alpha = 55^\circ$ ,

with a ratio of 3.43, whereas the ratio is not greater than 1.4 at  $\alpha = 85^\circ$ .

Fig. 19 shows the effect of using the three different proposed  $K$  parameters:  $K_o$ ,  $K_a$  and  $K_{a\beta}$  on the determination of standardised vertical stress for different internal friction angles  $\phi$ , with  $\eta = 0.5$  and  $\alpha = 70^\circ$ . It was found that the ratio between the maximum and minimum normalised vertical stresses was not greatly affected by the internal friction angle  $\phi$ . The maximum ratio was 1.4 for  $\phi = 30^\circ$ , 1.45 for  $\phi = 35^\circ$  and 1.5 for  $\phi = 40^\circ$ , as indicated in Fig. 19a, b and c, respectively.

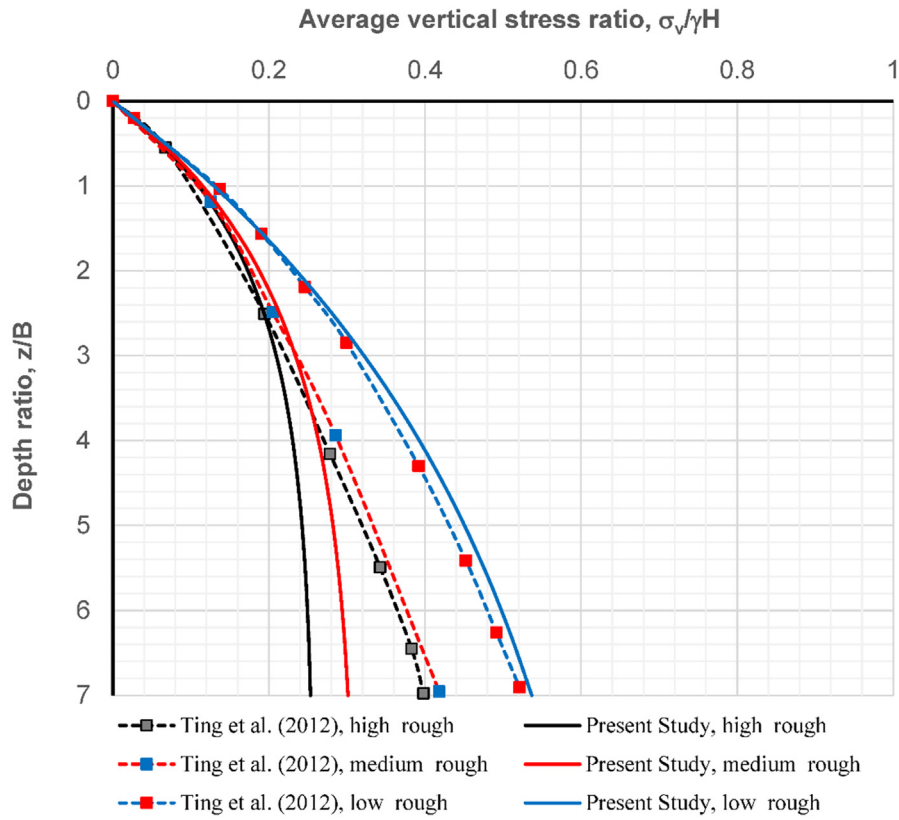


**Fig. 13** Comparison of vertical stresses along the vertical centreline for specific stope aspect ratios (note that  $\alpha = 80^\circ$ ; in the present study  $K_0$  and  $\eta = 0.8$  were used, with  $\phi = 40^\circ$ ).

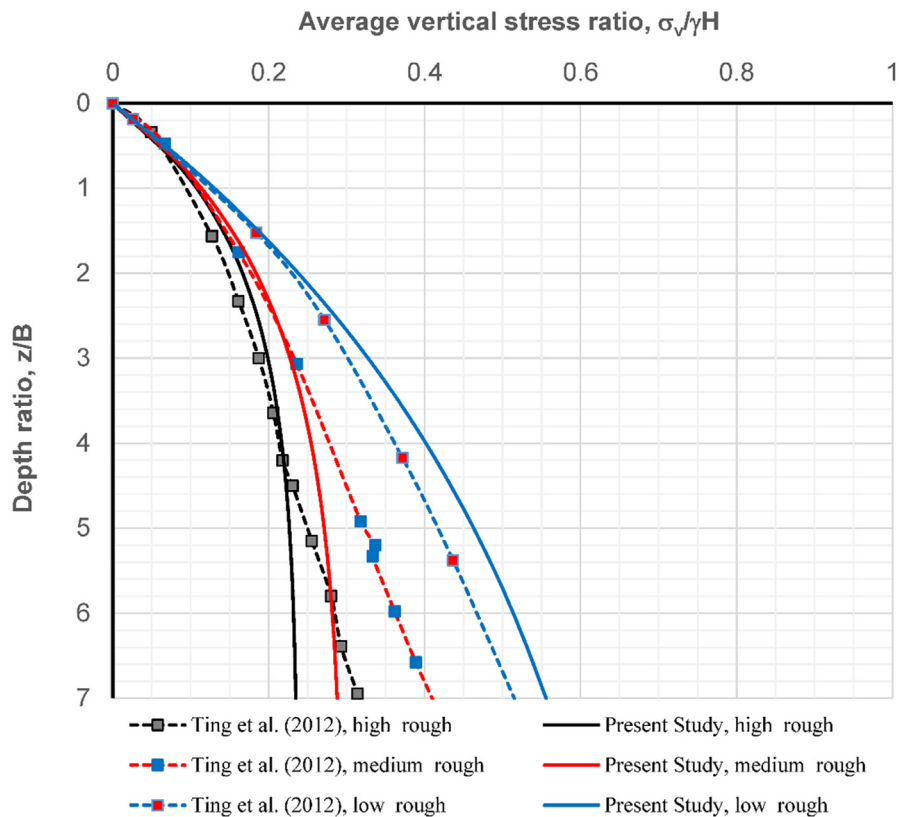


**Fig. 14** Comparison of vertical stresses along the vertical centreline for specific stope aspect ratios (note that  $\alpha = 90^\circ$ ; in the present study  $K_0$  and  $\eta = 1.0$  were used, with  $\phi = 40^\circ$ ).

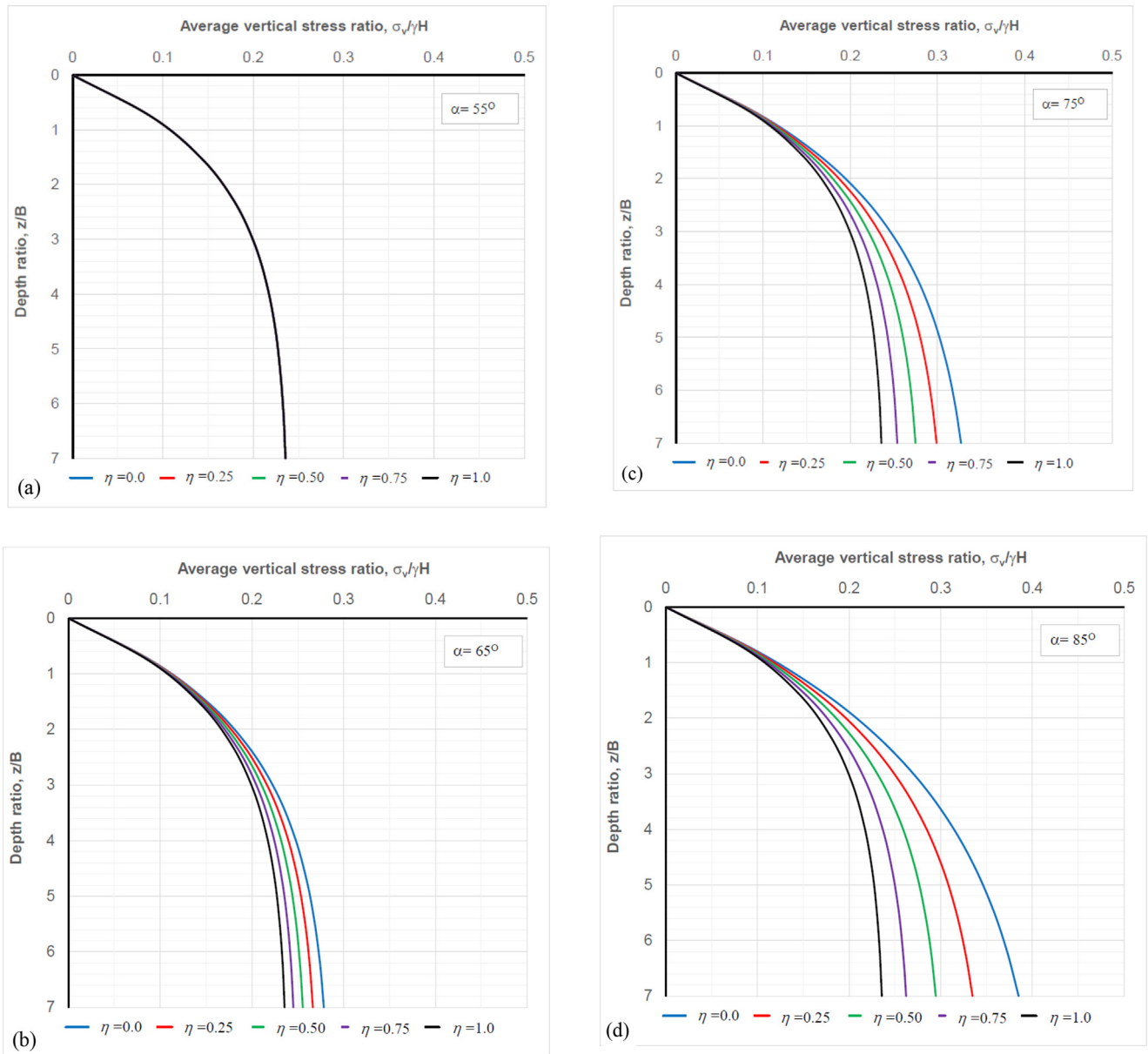


**Fig. 15** The effect of  $\eta$  on the normalised vertical stress at different stope angles of inclination, for  $K = K_o$ , with a high roughness interface friction angle and  $\phi = 35^\circ$ .

**Fig. 15** (continued)

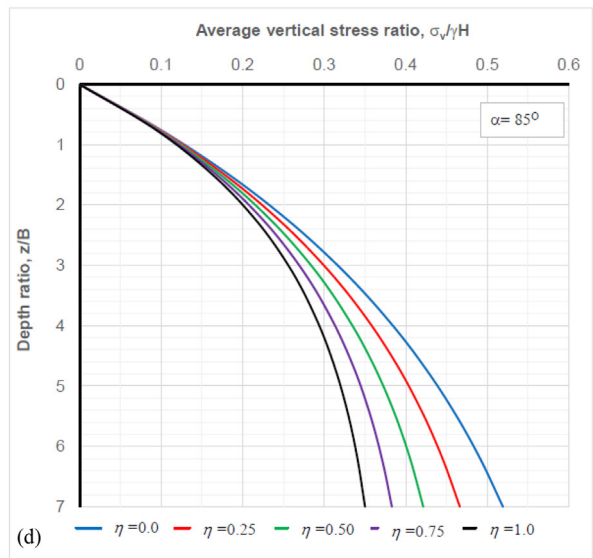
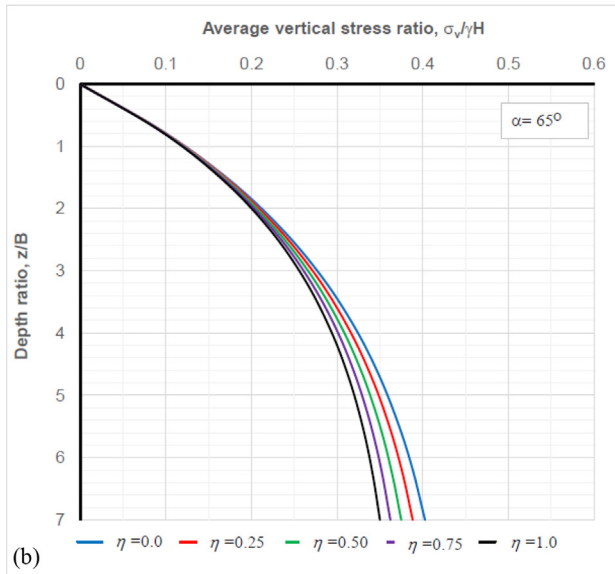
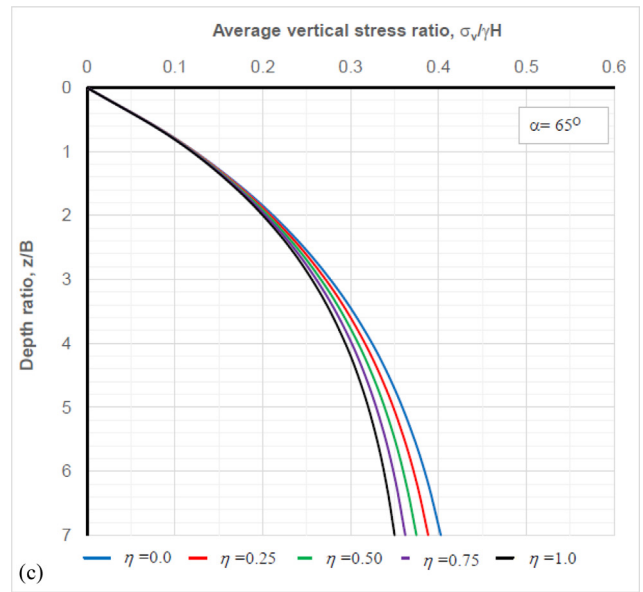
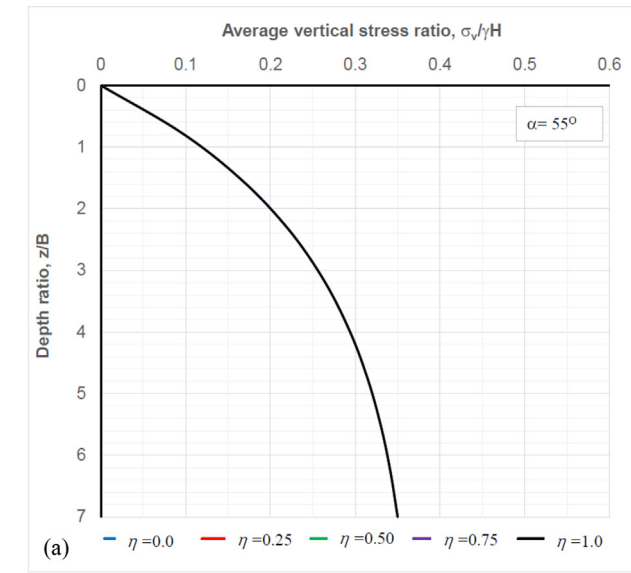


**Fig. 16** The effect of  $\eta$  on the normalised vertical stress at different stope angles of inclination, for  $K = K_a$ , with a high roughness interface friction angle and  $\phi = 35^\circ$ .

**Fig. 16** (continued)

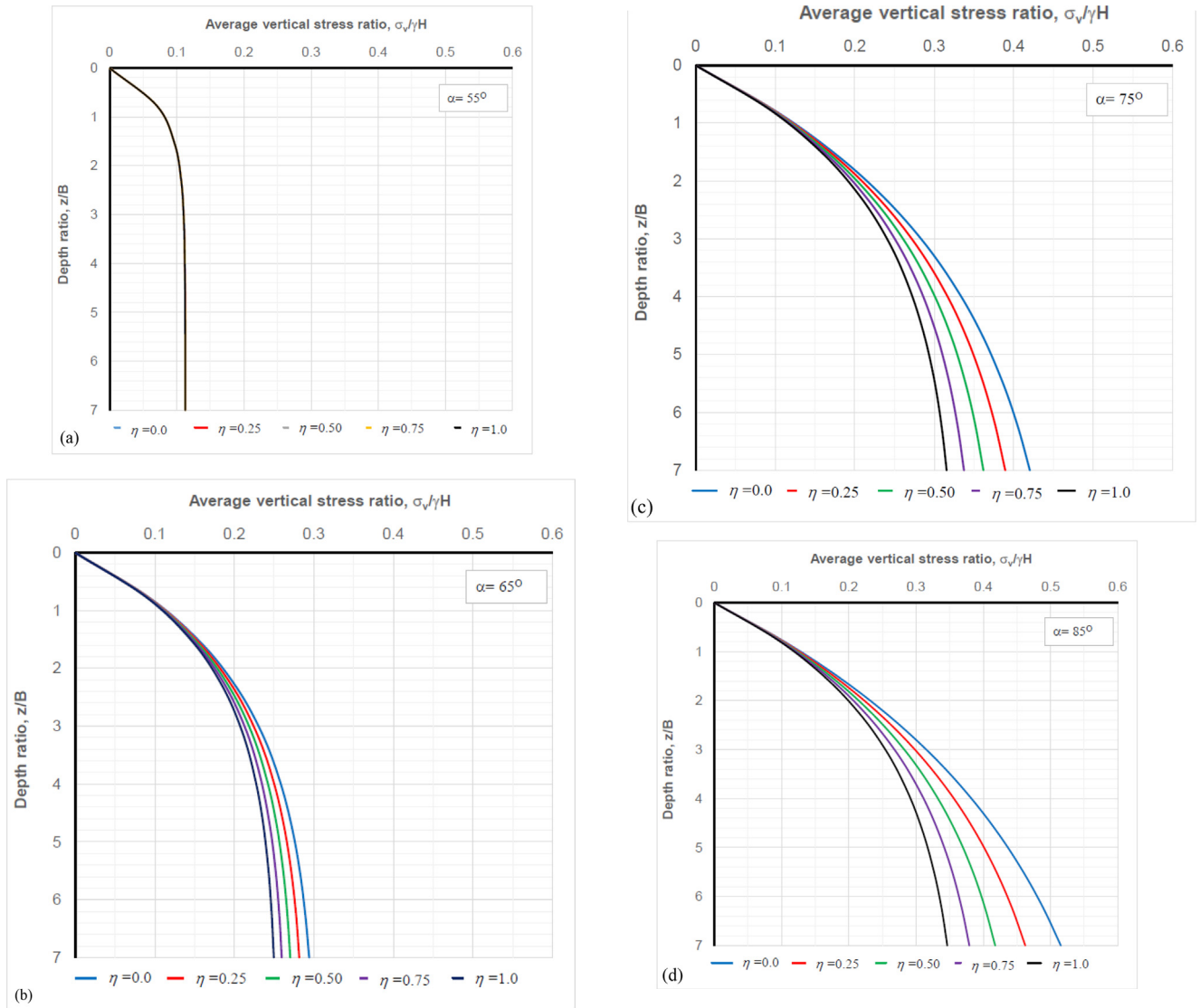
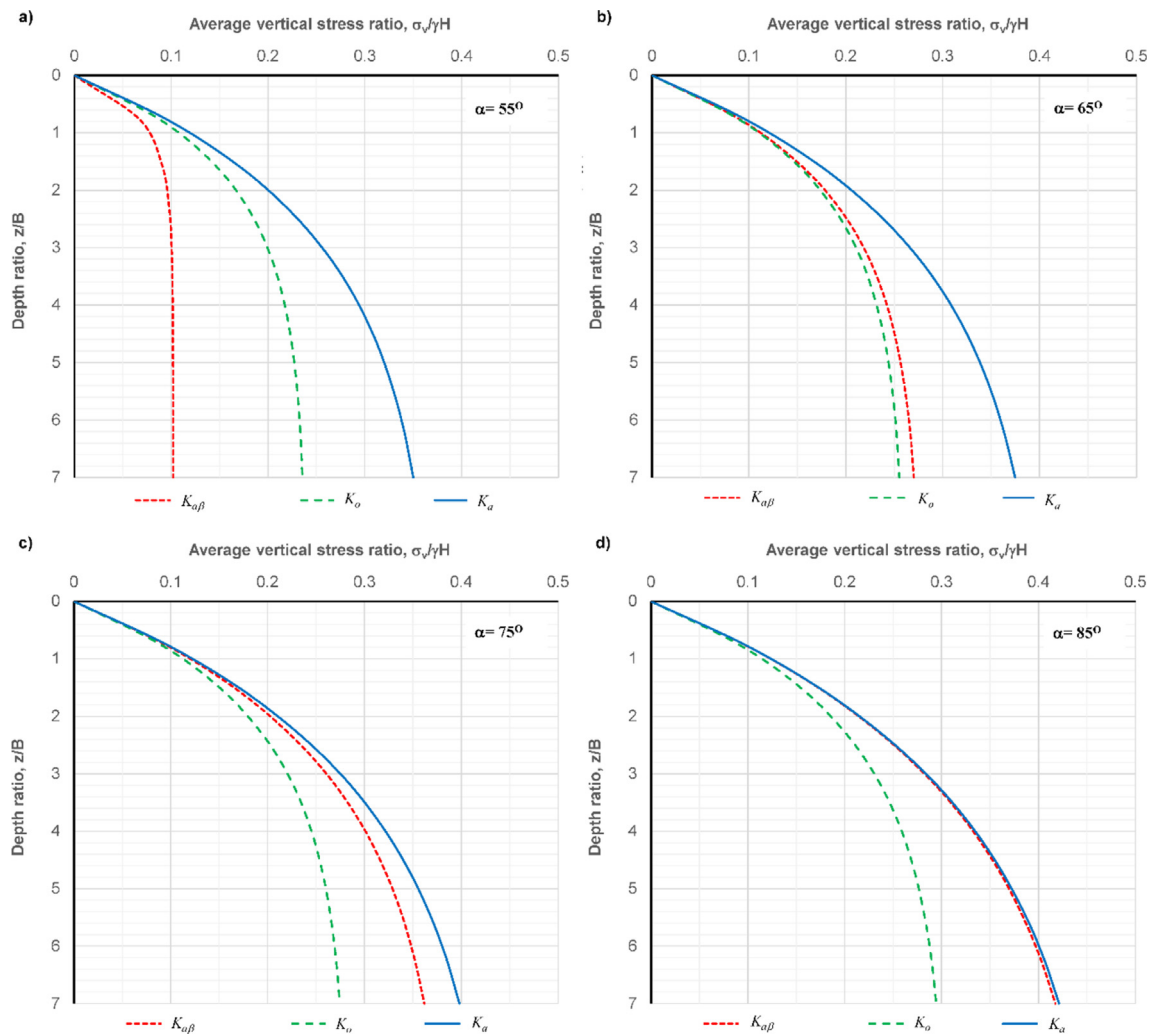


Fig. 17 (continued)

**Fig. 17** The effect of  $\eta$  on the normalised vertical stress at different stope angles of inclination, for  $K = K\alpha\beta$ , with a high roughness interface friction angle and  $\phi = 35^\circ$ .



**Fig. 18** The effect of K parameters on the normalised vertical stress at different stope angles of inclination, with a high roughness interface friction angle,  $\phi = 35^\circ$  and  $\eta = 0.5$ .

## 6. Conclusions

The following conclusions can be drawn based on the findings discussed above.

- A proposed new formula based on Marston's theory is used to determine the vertical stress at any depth in backfilled inclined mine stopes, taking into account the impact of arching on the backfill material. The proposed formula is limited to two-dimensional plane strain applications and requires a large stope height/width ratio.
- For the proposed formula, it is suggested that the normal stress reaction on the hanging wall could be adjusted as a percentage of the normal stress on the footwall. The resulting parameter,  $\eta$ , would thus permit the proposed formula to be suitable for different inclined mine stope situations.
- Results of the proposed formula are compared to the results of laboratory experiments, and good agreement is also found with the results of previously developed analytical expressions and numerical studies.
- For the proposed formula, parametric studies are carried out for the reaction ratio between the hanging wall and footwall, expressed by  $\eta$ , as well as for the coefficient of lateral earth pressure,  $K$ .
- As compared to the case where  $\eta = 0$ , the use of  $\eta = 1$  results in a 61 to 67% reduction in vertical stress at the base of the stope. This is attributable to the effect of the arching phenomenon in inclined mine stopes. Furthermore, higher height/width ( $z/B$ ) stope aspect ratios are associated with greater variation in the normalised vertical stress, depending on the value of  $\eta$ . The arching effect is found to be less important for lower height/width aspect ratios, and the stress exerted at the bottom of the stope is almost independent of  $\eta$  when  $z/B$  less than 1.5.

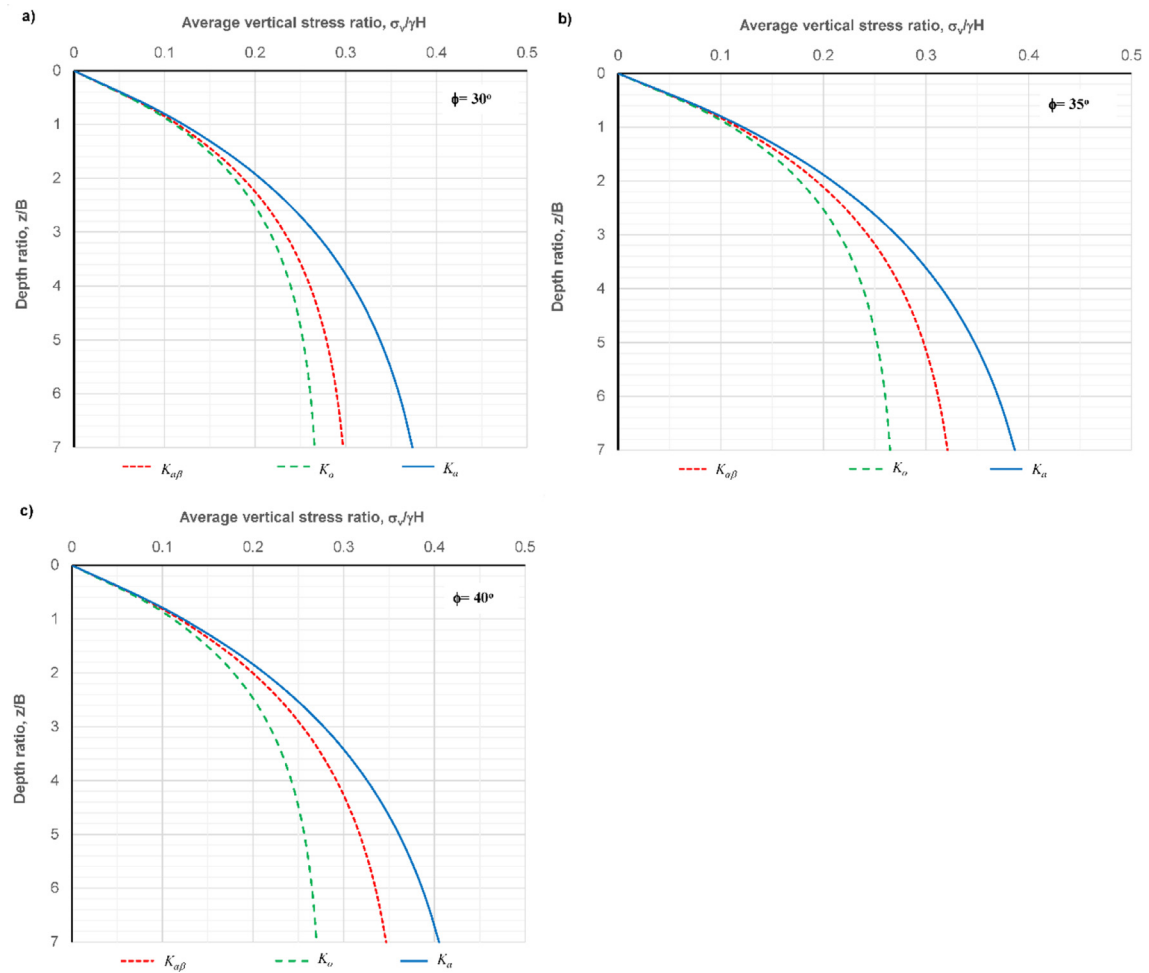


**Fig. 19** The effect of K parameters on the normalised vertical stress for various backfill internal friction angles, with a high roughness interface friction angle,  $\alpha = 700$  and  $\eta = 0.5$ .

- Comparisons with previous results indicate that for  $K = K_0$ , the most acceptable value for  $\eta$  is 0.6. However, the use of  $\eta = 0.3$  and  $\eta = 0.9$  yields good agreement with experimental data where  $K = K_\alpha$  and  $K = K_{\alpha\beta}$ , respectively.
- The guideline results show that using the coefficient  $K_0$  with  $\eta = 0.6$  is appropriate for all slope angles of inclination less than  $90^\circ$ , whereas using  $K_\alpha$  with  $\eta = 0.3$  is recommended for vertical mine stopes.

## 7. Data availability

All data, models, and code generated or used during the study appear in the submitted article.

## Declaration of Competing Interest

The authors declare that they have no known competing financial interests or personal relationships that could have appeared to influence the work reported in this paper. The research has received no funding. The research was conducted while completing a postdoctoral fellowship at James Cook University.

## References

- [1] A.C. Adoko, K. Yakubov, A. Alipov, Mine stope performance assessment in unfavorable rock mass conditions using neural network-based classifiers. In 5th ISRM Young Scholars' Symposium on Rock Mechanics and International Symposium on Rock Engineering for Innovative Future. OnePetro (2019, December).
- [2] M. Aubertin, L.S.T.B.M. Li, S. Arnoldi, T. Belem, B. Bussi re, M. Benzaazoua, R. Simon, Interaction between backfill and rock mass in narrow stopes, *Soil and rock America* 1 (2003) 1157–1164.
- [3] A.W. Bishop, Test requirements for measuring the coefficient of earth pressure at rest, British Library Lending Division [supplier], 1958.
- [4] L.E. Bowles, *Foundation analysis and design*, McGraw-hill, 1996.
- [5] C.A. Caceres Doerner, Effect of delayed backfill on open stope mining methods, University of British Columbia, 2005, Doctoral dissertation.
- [6] M.C. Bridges, A new era of fill-retaining barricades. AMC's newsletter "Digging Deeper" on current events and modern mining methodology. 2003.
- [7] W. El Kamash, H. El Naggat, S. Nagaratnam, Numerical analysis of lateral earth pressure coefficient in inclined mine

- stopes, *Geomechanics and Geophysics for Geo-Energy and Geo-Resources* 7 (3) (2021) 1–24.
- [8] M.A. El-Sohby, K.Z. Andrawes, Deformation characteristics of granular materials under hydrostatic compression, *Canadian Geotechnical Journal* 9 (4) (1972) 338–350, <https://doi.org/10.1139/t72-038>.
- [9] M. Fahey, M. Helinski, A. Fourie, Some aspects of the mechanics of arching in backfilled stopes, *Canadian Geotechnical Journal* 46 (11) (2009) 1322–1336, <https://doi.org/10.1139/T09-063>.
- [10] R.L. Handy, The arch in soil arching, *Journal of Geotechnical Engineering* 111 (3) (1985) 302–318, [https://doi.org/10.1061/\(ASCE\)0733-9410\(1985\)111:3\(302\)](https://doi.org/10.1061/(ASCE)0733-9410(1985)111:3(302)).
- [11] R.L. Handy, M. Spangler, M.G. Spangler, *Geotechnical engineering: soil and foundation principles and practice*, McGraw Hill (2007), Professional.
- [12] J. Jaky, Pressure in silos. *Proc. 2nd ICSM, 1948* (1948).
- [13] S. Knutsson, Stresses in the hydraulic backfill from analytical calculations and in-situ measurements. In *Conference on the Application of Rock Mechanics to Cut and Fill Mining: 01/06/1980-03/06/1980* (pp. 261-268). The Institution of Mining and Metallurgy (1981).
- [14] L.i. Li, M. Aubertin, An analytical solution for the nonlinear distribution of effective and total stresses in vertical backfilled stopes, *Geomechanics and Geoengineering* 5 (4) (2010) 237–245.
- [15] L. Li, M. Aubertin, Horizontal pressure on barricades for backfilled stopes. Part I: Fully drained conditions, *Canadian Geotechnical Journal* 46 (1) (2009) 37–46, <https://doi.org/10.1139/T08-104>.
- [16] L. Li, M. Aubertin, R. Simon, B. Bussi ere, T. Belem, Modeling arching effects in narrow backfilled stopes with FLAC, in: *In FLAC and numerical modelling in geomechanics-2003*, 2003, pp. 211–219.
- [17] L. Li, M. Aubertin, T. Belem, Formulation of a three dimensional analytical solution to evaluate stresses in backfilled vertical narrow openings, *Canadian Geotechnical Journal* 42 (6) (2005) 1705–1717, <https://doi.org/10.1139/t05-084>.
- [18] L.i. Li, M. Aubertin, An improved analytical solution to estimate the stress state in subvertical backfilled stopes, *Canadian Geotechnical Journal* 45 (10) (2008) 1487–1496.
- [19] L.i. Li, M. Aubertin, Numerical investigation of the stress state in inclined backfilled stopes, *International Journal of Geomechanics* 9 (2) (2009) 52–62.
- [20] A. Marston, The theory of external loads on closed conduits in the light of the latest experiments. In *Highway research board proceedings* (Vol. 9) (1930).
- [21] A. Marston, The theory of loads on pipe in ditches and tests of cement and clay drain tile and sewer pipe, *Bulletin* 31 (1913).
- [22] D.F. McCarthy, D.F. McCarthy, *Essentials of soil mechanics and foundations*, Vol. 505, Reston Publishing Company, Virginia, 1977.
- [23] R.J. Mitchell, R.S. Olsen, J.D. Smith, Model studies on cemented tailings used in mine backfill, *Canadian Geotechnical Journal* 19 (1) (1982) 14–28.
- [24] M. Nujaim, T. Belem, A. Giraud, Experimental Tests on a Small-Scale Model of a Mine Stope to Study the Behavior of Waste Rock Barricades during Backfilling, *Minerals* 10 (11) (2020) 941.
- [25] K. Pirapakaran, N. Sivakugan, Arching within hydraulic fill stopes, *Geotechnical and Geological Engineering* 25 (1) (2007) 25–35, <https://doi.org/10.1007/s10706-006-0003-6>.
- [26] K. Pirapakaran, N. Sivakugan, Pirapakaran, K., and N. Sivakugan. "Numerical and experimental studies of arching effects within mine fill slopes. *James Cook Conference Item (Research - E1)*, (2006) 1519-1525.
- [27] K. Pirapakaran, N. Sivakugan, A laboratory model to study arching within a hydraulic fill stope, *Geotechnical Testing Journal* 30 (6) (2007) 496–503.
- [28] K.J. Rankine, N. Sivakugan, R. Cowling, Emplaced geotechnical characteristics of hydraulic fills in a number of Australian mines, *Geotechnical & Geological Engineering* 24 (1) (2006) 1–14.
- [29] M.B. Revell, D.P. Sainsbury, Advancing paste fill bulkhead design using numerical modeling. In *International Symposium of MineFill07, Montreal* (2007, April).
- [30] A. Saeidi, S. Heidarzadeh, S. Lalancette, A. Rouleau, The effects of in situ stress uncertainties on the assessment of open stope stability: Case study at the Niobec Mine, Quebec (Canada), *Geomechanics for Energy and the Environment* 25 (2021) 100194, <https://doi.org/10.1016/j.gete.2020.100194>.
- [31] S. Singh, S.K. Shukla, N. Sivakugan, Arching in inclined and vertical mine stopes, *Geotechnical and Geological Engineering* 29 (5) (2011) 685–693.
- [32] S. Singh, N. Sivakugan, S.K. Shukla, Can soil arching be insensitive to  $\phi$ ?, *International Journal of Geomechanics* 10 (3) (2010) 124–128.
- [33] N. Sivakugan, S. Widinghe, Stresses within granular materials contained between vertical walls, *Indian Geotechnical Journal* 43 (1) (2013) 30–38.
- [34] M.A. Sobhi, L.i. Li, M. Aubertin, Numerical investigation of earth pressure coefficient along central line of backfilled stopes, *Canadian Geotechnical Journal* 54 (1) (2017) 138–145.
- [35] K. Terzaghi, R.B. Peck, G. Mesri, *Soil mechanics in engineering practice*, John Wiley & Sons, 1996.
- [36] C.H. Ting, S.K. Shukla, N. Sivakugan, Arching in soils applied to inclined mine stopes, *International Journal of Geomechanics* 11 (1) (2011) 29–35.
- [37] C.H. Ting, N. Sivakugan, S.K. Shukla, Laboratory simulation of the stresses within inclined stopes, *Geotechnical Testing Journal* 35 (2) (2012) 280–294.
- [38] J.A. Vallejos, A. Delonca, E. Perez, Three-dimensional effect of stresses in open stope mine design, *International Journal of Mining, Reclamation and Environment* 32 (5) (2018) 355–374.
- [39] M.E. Villalba Matamoros, M. Kumral, Underground mine planning: stope layout optimisation under grade uncertainty using genetic algorithms, *International Journal of Mining, Reclamation and Environment* 33 (5) (2019) 353–370.
- [40] P. Yang, L. Li, M. Aubertin, Stress ratios in entire mine stopes with cohesionless backfill: A numerical study, *Minerals* 7 (10) (2017) 201.
- [41] X.J. Yang, F. Gao, Y. Ju, H.W. Zhou, Fundamental solutions of the general fractional-order diffusion equations, *Mathematical Methods in the Applied Sciences* 41 (18) (2018) 9312–9320.